Electrochemical and Solid-State Letters, **8** (3) C58-C61 (2005)
1099-0062/2005/8(3)/C58/4/$7.00 © The Electrochemical Society, Inc.

Electroplating of Ni_4W

T. M. Sridhar,[a] N. Eliaz,[a,*,z] and E. Gileadi[b,]**

[a]*Biomaterials and Corrosion Laboratory, Department of Solid Mechanics, Materials and Systems, Tel-Aviv University, Ramat-Aviv 69978, Israel*
[b]*School of Chemistry, Raymond and Beverly Sackler Faculty of Exact Sciences, Tel-Aviv University, Ramat-Aviv 69978, Israel*

Nickel-tungsten alloys were electrodeposited on stationary working electrodes from a nickel sulfate, sodium tungstate, and tri-sodium citrate-based bath under different operating conditions. The microstructure of the deposits was studied by X-ray diffraction, the morphology by scanning electron microscopy and atomic force microscopy, and the approximate composition by energy dispersive spectroscopy. Different Ni-W phases, either amorphous or crystalline, were associated with different plating conditions. A body-centered tetragonal Ni_4W phase was formed only at high temperatures and low current density. This is the first time that the formation of this phase by electroplating was observed repeatedly.
 [DOI: 10.1149/1.1857114]

Manuscript submitted September 4, 2004; revised manuscript received November 24, 2004. Available electronically January 24, 2005.

Interest in electrodeposition of nickel-tungsten (Ni-W) alloys has increased in recent years due to their unique combination of tribological, magnetic, electrical, and electro-erosion properties. Tungsten cannot be electrodeposited from an aqueous solution of sodium tungstate (Na_2WO_4) or any other soluble compound containing this element. However, if a suitable nickel compound, such as nickel sulfate ($NiSO_4$), is added to the plating bath, induced codeposition can take place, forming Ni-W alloys. The use of citrate as a ligand and exclusion of ammonia from the bath allows for a significant increase of the tungsten concentration in the alloy.[1]

Recently, the authors reviewed literature on electrodeposition of Ni-W alloys and studied the effect of Ni^{2+}, Cit^{3-}, bath additives, applied current density, and bath temperature on the Faradaic efficiency (FE), tungsten content, and properties of Ni-W alloys deposited on stationary working electrodes.[1] The objective of this work was to demonstrate the sensitivity of the obtained deposit microstructure to operating conditions and to show that a Ni_4W phase can be formed electrochemically.

Experimental

Nickel-tungsten alloys were electroplated from aqueous solutions containing 0.10 M nickel sulfate, 0.40 M sodium tungstate, and 0.50 M tri-sodium citrate. All reagents were dissolved in Simplicity water. The pH was adjusted to a value of 8.0 by additions of H_2SO_4 and NaOH. No additives were used.

A two-electrode cell was used. A sheet of gold with an exposed area of 1 cm^2 was used as the cathode (working electrode). A platinum mesh was used as the anode (counter electrode) and was placed 10 mm away from the cathode. The anode-to-cathode surface area ratio was ~4.4, high enough to minimize polarization of the anode and an increase in the voltage drop between the two electrodes. A Keithley model 2425 source meter was used to control the applied current density at 5 mA/cm^2 (unless otherwise stated). Before turning on the current, the bath was purged with purified nitrogen for about 15 min. Purging continued during deposition. The plating bath was operated at different temperatures, from room temperature to 70°C. A Lauda Ecoline E-220T thermostatic bath was used to control the temperature to within ±0.01°C. To maintain homogeneity of the solution and reduce pitting due to accumulation of hydrogen at the surface of the cathode, vigorous stirring at 1500 rpm was maintained during plating, employing a flat magnetic stirrer. Electroplating was conducted for 6 h, unless otherwise noted.

The structure of the deposits was analyzed by X-ray diffraction (XRD), employing a Θ-Θ powder diffractometer from Scintag, equipped with a liquid nitrogen-cooled germanium solid-state detector and Cu Kα radiation source (λ = 1.5406 Å). The morphology of the deposits after drying was observed with a scanning electron microscope (SEM, JEOL model JSM-6300). The attached energy dispersive spectroscopy (EDS, Oxford Isis system) was used to determine the approximate composition of the alloy. Several sessions were conducted with a field-emission high-resolution SEM (JEOL model JSM-6700F). Each sample was measured at different locations to confirm uniformity. *Ex situ* atomic force microscopy (AFM, using Molecular Imaging model PicoSPM operated under contact mode) was also used to analyze the structure of the deposits at near-atomic resolution.

Results and Discussion

Altogether, over 100 samples were coated in this project, under different bath chemistries and operating conditions. Representative samples, of interest to the discussion here, are listed in Table I. It should be recalled that in all cases, the nickel, tungstate and citrate ion concentrations were 0.10, 0.40, and 0.50 M, respectively. The phases in each deposit were determined by XRD in conjunction of EDS. Figure 1 shows several representative spectra.

The effect of plating bath temperature on the crystallographic structure of the deposit is evident from Fig. 1. The XRD patterns of Samples 89, 44, and 92 include a reflection which is consistent with the (211) strongest reflection of the body-centered tetragonal Ni_4W phase (JCPDS file no. 65-2673, Pearson symbol $tI10$, space group $I4/m$). Interestingly, the formation of this phase was identified only under conditions of low current density (5 mA/cm^2) and well above room temperature. From the XRD pattern of Sample 89 it seems that this phase starts forming at 50°C. Note that as the temperature is raised from 50 to 70°C, the $Ni_4W(211)$ reflection becomes more pronounced. EDS data (Table I) showed tungsten concentrations around 20 atom %, consistent with the formation of a Ni_4W phase. Any combination of raised temperature and higher current densities resulted in W concentrations in the range of 26-36 atom %, with no indication to the formation of Ni_4W by XRD (see, for example, data on sample 5). The halo noticed in the XRD patterns of samples 44 and 92 around $2\Theta = 50.4°$ may be related either to the Ni(200) reflection shifted due to W incorporation, or to the $Ni_4W(130)$ reflection. Generally, one would expect the halo to appear around the strongest reflection of the crystalline matrix phase. For crystalline Ni, this would be the (111) reflection at $2\Theta = 44.505°$ (JCPDS file no. 04-0850). However, because the Au substrate exhibits a (200) preferred orientation (see JCPDS file no. 04-0784), one cannot exclude the possibility that Ni is deposited on Au with a (200) preferred orientation as well. This reflection is found at $2\Theta = 51.844°$ for pure crystalline Ni. Thus, one may expect any amorphous Ni-based phase to appear around this angle, as claimed herein.

* Electrochemical Society Active Member.
** Electrochemical Society Fellow.
z E-mail: neliaz@eng.tau.ac.il

Table I. Plating parameters for selected samples.

Sample	T(°C)	i(mA/cm^2)	Faradaic efficiency (%)	Thickness (μm)	Alloy composition (atom % W)
5	RT	15	8	2.9 ± 0.7	31
89	50	5	16	8.7 ± 0.1	21
44	60	5	20	N/A	20
95	60	5	N/A	5.5 ± 0.3	20
92	70	5	21	5.9 ± 0.1	22

The surface morphologies of samples 44 and 95, which were plated under the same conditions, are shown in Fig. 2a and b, respectively. The morphology is not uniform, supporting the coexistence of an amorphous Ni-based phase and a crystalline Ni_4W phase. Figure 3a presents two-dimensional topography, Fig. 3b two-dimensional deflection, and Fig. 3c three-dimensional topography AFM images of sample 95. The scan area here is 4.75 × 4.75 μm. The deflection image, also known as the error signal image, results from the inability of the electronics feedback circuit to maintain a constant force. This represents the gradient of shape change via differentiation, and is thus more sensitive to delegate spatial information such as sharp edges. A scan along the line marked in Fig. 3b yielded the profile given in Fig. 3d. The morphological periodicity, evident in both Fig. 3c and d, is consistent with our previous observation (Fig. 1) of a locally ordered crystalline structure. The aggregate periodicity is at distances of ~1.4 μm according to Fig. 3d. Note that no similar features were observed in AFM data on amorphous deposits.

The thickness and hardness of sample 89 were measured on a cross section and found to be 8.7 ± 0.1 μm and 668 ± 43 VHN, respectively. The deposit in sample 92 was thinner (5.9 ± 0.1 μm).[1] When the same plating conditions as for sample 44 were applied for longer 24 h (sample 96), the thickness of the deposit increased to 24.8 ± 0.6 μm, which allowed hardness measurement of 577 ± 44 VHN. Comparing this value to that for sample 89, one may conclude that by raising the bath temperature from 50 to 60°C, the hardness of the deposit decreased.[1] This observation is similar to that of Atanassov *et al.*,[2] who reported a maximum in hardness of about 720 VHN at 50°C under unstirred conditions.

Nasu *et al.*[3] have already compared the crystal structure of electrodeposited Ni-W alloys, as observed by small angle X-ray scattering (SAXS) and extended X-ray absorption fine structure (EXAFS)

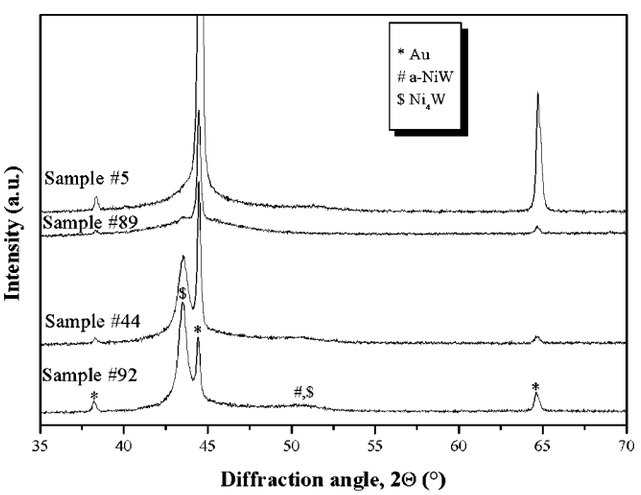

Figure 1. XRD spectra, demonstrating the effect of bath temperature on the structure of Ni-W electrodeposits. See Table I for further information.

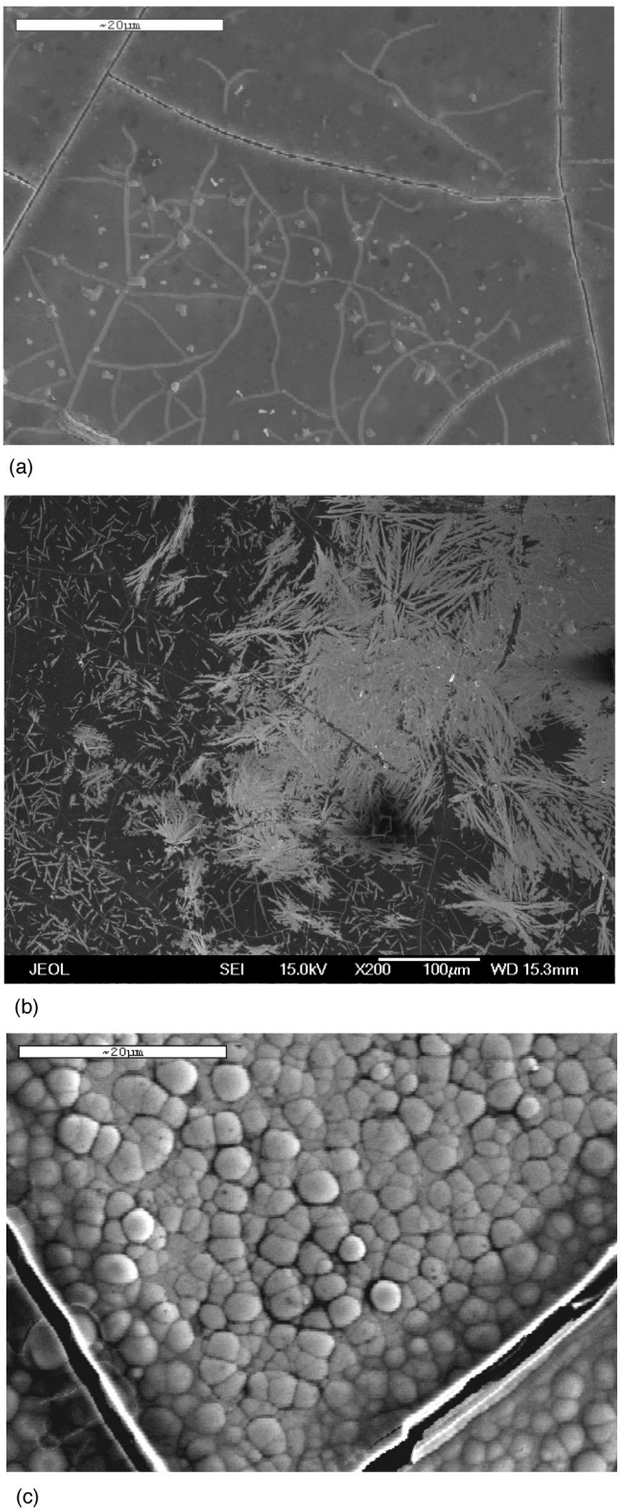

Figure 2. SEM secondary electron images, demonstrating the surface morphology of samples (a) 44, (b) 95, and (c) 5. See Table I for further information.

measurements, to that of Ni_4W predicted by a computer code. However, no experimental evidence for the formation of the Ni_4W compound was provided. Huang *et al.*,[4] on the other hand, did show by means of XRD and XPS that a Ni-W electrodeposit with a tungsten

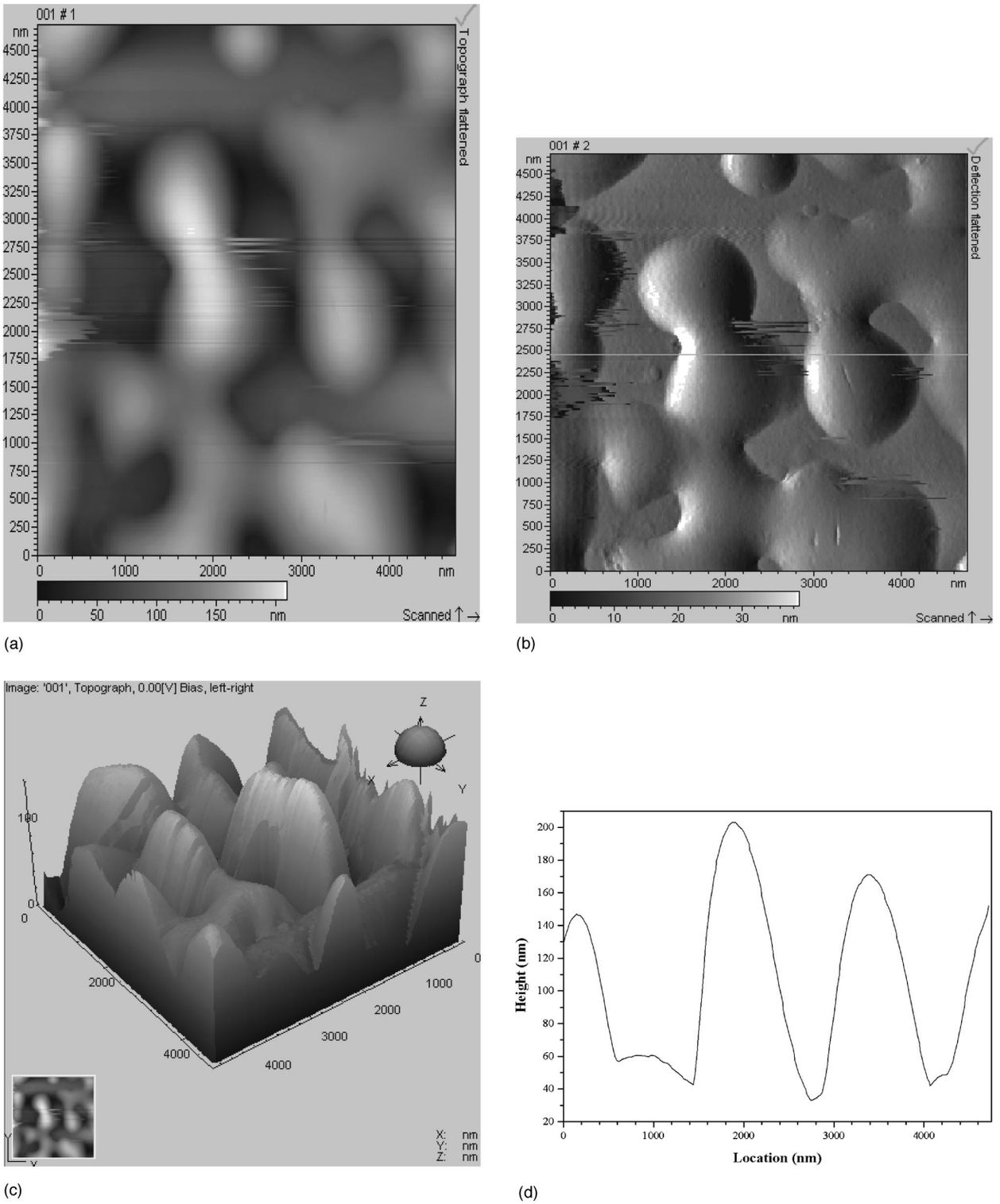

Figure 3. (a) Atomic force topography, (b) deflection, (c) 3D, and (d) line scan profile images of sample 95. The line along which scan was made is marked around $y = 2500$ nm in Fig. 3b.

content of about 18 atom % may consist of the intermetallic phase Ni_4W. Note that this phase, which had high hardness of 673 VHN, was formed at 60°C.[4]

In the present work it was found that, as the bath temperature was increased, the FE increased and the tungsten content decreased. A similar behavior was observed when the current density was decreased. Therefore, a combination of high temperature and low current density is expected to yield a relatively low tungsten concentration in the alloy, which would allow formation of the Ni_4W phase. To the best of our knowledge, this is the first systematic

observation of the formation of this phase electrochemically. Although the mechanism by which Ni_4W forms is not clear yet, its existence may support the claim that the compositions and microstructures of electrodeposited Ni-W alloys are strongly affected by the intermetallic compounds in the Ni-W system. Furthermore, because samples coated for 12 or 24 h at high temperature and low current density were typically more morphologically and chemically uniform compared to those coated for 6 h under the same conditions, it is possible that the reaction through which the Ni_4W phase is formed is time dependent (*i.e.*, kinetic constraints may play a role). This could have been one of the reasons for its absence in previous reports.

Before concluding, it may be of interest to discuss the other structures that were observed in the current work. First, the citrate concentration was found to have a distinct effect. When the sum of molar concentrations of $NiSO_4$ and Na_2WO_4 exceeded that of Na_3Cit, precipitation was observed in solution during deposition at room temperature. Although the composition of this crystalline precipitate was not studied in detail (EDS showed that it varied from 44 to 67 atom % W), it is assumed to be $NiWO_4$, which is known to be insoluble. Having an excess of complexing agent, either citrate or an ammonium salt, prevents the formation of this precipitate. In general, while any chemical composition around 50 atom % W may reflect a NiW phase, a concentration of about 66 atom % W would represent a NiW_2 phase. Younes *et al.* observed the formation of an orthorhombic NiW phase by XRD measurements (JCPDS file no. 47-1172, Pearson symbol o**), when the concentration of W in the deposit exceeded 40 atom %.[5,6] It was argued that formation of equal amounts of Ni and W in the alloy may be regarded as evidence, albeit circumstantial, for the existence of a tertiary nickel-tungstate-citrate complex. Later,[7] Younes *et al.* also reported the first plating of a body-centered tetragonal NiW_2 phase (Pearson symbol *tI*96, space group *I*4), with the same Bragg reflections as those for NiW.

In this work, when the citrate concentration was raised to 0.50 M at room temperature, the FE decreased and the structure of deposit changed significantly. Both XRD patterns and SEM images indicated the formation of an amorphous phase, either for low or high current density (see XRD pattern and SEM image of sample 5 in Fig. 1 and 2c, respectively). While the diffraction pattern shows distinct peaks related to the gold substrate (JCPDS file no. 04-0784), a halo is also noticed around $2\Theta = 51°$. This halo may represent either an amorphous or a fine nanocrystalline structure. Gileadi *et al.* have observed the formation of amorphous Ni-W alloys when the tungsten content fell within the range of 20-40 atom % (44-68 wt %).[5-7] Yamasaki *et al.*, too, reported the existence of amorphous structures in Ni-W alloys with tungsten content in excess of about 20 atom %.[8] This requirement is satisfied for sample 5, as evident from Table I. For amorphous materials, the distance between nearest neighbors can be calculated from the position of the halo maximum, according to the Debye equation. It was found[6] that, as more of the larger W atoms are incorporated into the amorphous structure, the halo is shifted slightly to lower diffraction angles, reflecting an increase in distance between nearest neighbors. This experimental shift may, in principal, be compared to that predicted theoretically based on the assumption of a substitutional solid solution of hard spheres. The halo observed for sample 5 is also shifted to a lower angle compared to the expected peak of pure Ni(200) at 51.84°.

An important question to consider is what motivates the formation of the metastable amorphous phase and by what mechanism is it formed. Gileadi *et al.*[6] argued that under sufficiently high overpotentials, almost all metal atoms reaching the surface are immediately discharged, making the formation of the (thermodynamically less stable) amorphous phase more favorable. If the deposition rate is high compared to the exchange rate, further layers of atoms will be formed before each layer has had the chance to assume its thermodynamically most stable crystalline structure by a dissolution/deposition exchange with the corresponding species in solution. In a subsequent paper,[7] the same authors explained that competition between two crystalline phases in a mixture could also give rise to the formation of an amorphous structure. Watanabe,[9] on the other hand, claimed that when the coordination numbers and atomic radii are markedly different, formation of an amorphous structure is favored. This should apply to the Ni-W system, where Ni has an fcc structure and an atomic radius of 1.246 Å, whereas W has a bcc structure and an atomic radius of 1.408 Å (*i.e.*, 13% larger than that of Ni).

Conclusions

This work demonstrated the synergistic effect of low current density and high bath temperature on the structure of Ni-W alloys electrodeposited on stationary working electrodes in well-stirred solutions. All plating baths consisted of nickel sulfate, sodium tungstate, and tri-sodium citrate. The FE increased as either the current density decreased or the temperature increased. Different Ni-W phases, either amorphous or crystalline, were associated with different plating conditions. At sufficiently high citrate concentrations, an amorphous Ni-W phase formed at room temperature and different current densities. At elevated temperatures (50-70°C) and low current density, reproducible formation of the body-centered tetragonal Ni_4W phase was observed.

Acknowledgments

The authors thank M. Eliyahu for his help with AFM measurements. We also thank Dr. Yu. Rosenberg from the Wolfson Applied Materials Research Center, Tel-Aviv University, for performing the XRD measurements and helping in the analysis of the data. T.M.S. is thankful to the Pikovsky Valachi Foundation, Tel Aviv University, for providing him with a postdoctoral scholarship.

References

1. N. Eliaz, T. M. Sridhar, and E. Gileadi, *Electrochim. Acta*, In press.
2. N. Atanassov, K. Gencheva, and M. Bratoeva, *Plat. Surf. Finish.*, **84**, 67 (1997).
3. T. Nasu, M. Sakurai, T. Kamiyama, T. Usuki, O. Uemura, and T. Yamasaki, *J. Non-Cryst. Solids*, **312-314**, 319 (2002).
4. L. Huang, J. X. Dong, F. Z. Yang, S. K. Xu, and S. M. Zhou, *Trans. IMF*, **77**, 185 (1999).
5. O. Younes and E. Gileadi, *Electrochem. Solid-State Lett.*, **3**, 543 (2000).
6. O. Younes, L. Zhu, Y. Rosenberg, Y. Shacham-Diamand, and E. Gileadi, *Langmuir*, **17**, 8270 (2001).
7. O. Younes-Metzler, L. Zhu, and E. Gileadi, *Electrochim. Acta*, **48**, 2551 (2003).
8. T. Yamasaki, R. Tomohira, Y. Ogino, P. Schloßmacher, and K. Ehrlich, *Plat. Surf. Finish.*, **87**, 148 (2000).
9. T. Watanabe, *Mater. Sci. Eng., A*, **179/180**, 193 (1994).